

Optically selected fossil groups; X-ray observations and galaxy properties

Habib G. Khosroshahi^{1*}, Ghassem Gozaliasl^{2,3}, Jesper Rasmussen⁴,
Alireza Molaeinezhad¹, Trevor Ponman⁵, Ali A. Dariush⁶, Alastair J.R. Sanderson⁵

¹*School of Astronomy, Institute for Research in Fundamental Sciences (IPM), P. O. Box 19395-5746, Tehran, Iran*

²*School of Physics, Tabriz University, Tabriz, Iran*

³*Department of Physics, University of Helsinki, P. O. Box 64, FI-00014 Helsinki, Finland*

⁴*Dark Cosmology Centre, Niels Bohr Institute, University of Copenhagen, Juliane Maries Vej 30, DK-2100 Copenhagen, Denmark*

⁵*School of Physics and Astronomy, University of Birmingham, Birmingham B15 2TT, UK*

⁶*Institute of Astronomy, University of Cambridge, Madingley Road, Cambridge CB3 0HA, UK*

16 June 2014

ABSTRACT

We report on the X-ray and optical observations of galaxy groups selected from the 2dfGRS group catalog, to explore the possibility that galaxy groups hosting a giant elliptical galaxy and a large optical luminosity gap present between the two brightest group galaxies, can be associated with an extended X-ray emission, similar to that observed in fossil galaxy groups. The X-ray observations of 4 galaxy groups were carried out with *Chandra* telescope with 10–20 *ksec* exposure time. Combining the X-ray and the optical observations we find evidences for the presence of a diffuse extended X-ray emission beyond the optical size of the brightest group galaxy. Taking both the X-ray and the optical criteria, one of the groups is identified as a fossil group and one is ruled out because of the contamination in the earlier optical selection. For the two remaining systems, the X-ray luminosity threshold is close to the convention know for fossil groups. In all cases the X-ray luminosity is below the expected value from the X-ray selected fossils for a given optical luminosity of the group. A rough estimation for the comoving number density of fossil groups is obtained to be 4 to $8 \times 10^{-6} \text{ Mpc}^{-3}$, in broad agreement with the estimations from observations of X-ray selected fossils and predictions of cosmological simulations.

Key words: galaxies: clusters: general galaxies: elliptical and lenticular, cD galaxies: haloes intergalactic medium X-ray: galaxies X-rays: galaxies: clusters.

1 INTRODUCTION

Fossil groups (Ponman et al. 1994) are galaxy groups dominated by a single giant elliptical galaxy, some as luminous as brightest cluster galaxies (BCG). Formally, fossil groups are identified as having X-ray luminosities comparable to X-ray bright groups ($L_X \geq 10^{42} \text{ erg s}^{-1}$) and a difference of 2 magnitude or more between the first and second ranked galaxies within half the group Virial radius (Jones et al. 2003). The physically origin of fossil galaxy groups is argued to be in galaxy mergers. The X-ray observations of galaxy groups show that some of these groups have substantial amount of group scale X-ray emission which itself indicates deep gravitational potential of dark matter. This indicates that the hot gas is retained during the process of galaxy mergers.

There are now tens of fossil groups identified (Khosroshahi, Jones & Ponman 2004; Sun et al. 2004; Ulmer et al. 2005; Khosroshahi, et al 2006; Santos et al. 2007) observationally mostly meeting the criteria introduced by Jones et al. (2003). Due to their observationally distinct properties relative to the general population of galaxy groups, they are believed to be suitable systems to study the formation and evolution of giant elliptical galaxies (Khosroshahi, Ponman & Jones 2006; Smith et al. 2010) and galaxy groups and clusters (Khosroshahi, Ponman & Jones 2007; Dariush et al. 2007). Our earlier *Chandra* study of a small sample of fossil groups (Khosroshahi, Ponman & Jones 2007) shows several interesting features. The X-ray morphology of fossils is undisturbed indicating the absence of recent major merger. The dominant galaxy lies at the centre of group-scale X-ray emission, which traces the dark matter potential well. In ad-

* E-mail: habib@ipm.ir

dition, fossils are over-luminous in X-rays, for their optical luminosity, but fall comfortably on the standard $L_X - T_X$ relation Khosroshahi, Ponman & Jones (2007) suggesting that their hot gas temperature may also be elevated. The dark matter distribution in fossil groups is more centrally concentrated than in other groups and clusters, indicating early formation epoch for fossils. The differences between fossils and non-fossil groups are not limited to their hot gas and dark matter. The dominant central galaxies in fossils have disky or pure elliptical isophotes, while the majority of giant elliptical galaxies, and BCGs in particular, have boxy isophotes (Khosroshahi, Ponman & Jones 2006; Smith et al. 2010).

The observed properties of fossil groups point to their early formation and lack of later disturbance. Thus they must be amongst the first systems to have been virialized, which makes them very important probes of the early Universe. In many respects they should be similar to the cores of clusters, but with the distinction that fossil groups have not been subject to the subsequent subcluster merging which leads to the growth of galaxy clusters. These distinctive characteristics makes fossil groups especially valuable as a check on the adequacy of cosmological simulations. We have shown, using the Millennium simulations (Springel et al. 2005), that galaxy groups with large luminosity gaps are formed relatively earlier than groups with least luminosity gap between the two brightest galaxies (Dariush et al. 2007, 2010). Also fossils are seen as suitable environments to study IGM heating and cooling in the absence of group scale mergers (Miraghaee et al. 2013). The luminosity gap as an observable quantity for a galaxy group is also shown to be a strong probe of galaxy formation and evolution models (Tavassoli et al. 2010; Gozaliasl et al. 2013).

The primary aim of this study is to test the hypothesis that most of the galaxy merging which builds up giant elliptical galaxies actually takes place in collapsed groups. If this hypothesis is true, one could also expect that a great majority of purely optically selected fossil groups, e.g. groups with large luminosity gap between the two brightest members, to show group-scale X-ray emission. If this turns out to be true, it would result in a major advance in understanding the formation of luminous elliptical galaxies. In addition it would significantly raise the number of known fossil groups, and establish an economical and efficient method for finding more such systems.

To achieve this, we carried out *Chandra* observations aimed at detecting X-ray emission from optically selected groups. Rasmussen et al (2006) adapted a similar approach using the *XMM-Newton* and found low X-ray luminosity ($L_X \approx 10^{40} \text{ erg s}^{-1}$) in several groups which were selected at random from the 2dFGRS to have group velocity dispersion, $\sigma_v \approx 300 \text{ km s}^{-1}$. They argued that their groups may have not been fully collapsed, as an explanation of their findings. However, their sample had no constraint on the brightest group galaxy luminosity/morphology or on the magnitude gap between the two most luminous member galaxies, which feature in our selection of galaxy groups.

In this contribution, we report on the X-ray and the optical observations of the sample. Section 2 describes our sample selection and observation strategy, the X-ray and the optical observations. Section 3 is dedicated to the X-ray analysis followed by optical properties of the groups and

the galaxy luminosity function in section 4. In section 5, a discuss of the results and our conclusions are given. $H_0 = 70 \text{ km s}^{-1} \text{ Mpc}^{-1}$ and $\Omega_m = 0.3$ are assumed throughout this paper.

2 SAMPLE SELECTION AND OBSERVATIONS

To address the question of whether optically selected groups dominated by luminous elliptical galaxies (e.g. groups with a large luminosity gap between the two brightest galaxies in the group), show any sign of group scale X-ray emission, we adapted the following sample selection strategy.

We draw galaxy groups from the 2PIGG catalogue of galaxy groups (Eke et al. 2004), based on the full release of 2dFGRS. We selected 2PIGG groups which satisfy the following criteria,

I. Groups with at least five confirmed members ($N_{gal} \geq 5$): This provides us with a more reliable estimate of the group velocity dispersion and reduces the danger of including groups of galaxies which are not physical associated.

II. Groups with magnitude difference between first and second ranked galaxies $\Delta M_{12} \geq 2.0$: This is the formal optical criterion for fossil groups, and is imposed to ensure that the L^* galaxies in groups have merged to form the central luminous galaxy.

III. Groups with a giant elliptical galaxy as the BGG: The study of the volume-limited sample of fossils (Jones et al 2003) showed that the brightest galaxy is always a giant elliptical. We therefore apply an absolute magnitude cut of $M_B < -21.5$ and choose only elliptical galaxies. Fig. 1 shows an example group.

Although the 2dF galaxy redshift survey, from which we selected our targets, reaches $z \approx 0.2$, the optical criteria $\Delta M_{12} \geq 2.0$ and $M_{bJ,BGG} \leq -21.5$, limit the depth of the volume to $z < 0.09$ within which the sample is complete. In addition, the $N_{gal} \geq 5$ criterion requires at least four non-brightest galaxies to be spectroscopically confirmed members of these groups. While this criterion does not add any additional constraint on the volume, the number of galaxy groups will be substantially reduced. From the 2PIGG catalog and within $z < 0.09$, we find that the trend in which the total number of galaxy groups decreases with increasing N_{gal} , is quite similar to the trend in which the number of groups with a large $\Delta M_{12} \geq 2$ decreases with N_{gal} . However, the number of groups with $\Delta M_{12} \geq 2$, for a given N_{gal} , is an order of magnitude smaller than the number of groups when this criterion is relaxed. This will be taken into account when we return to the estimation of the space density of fossil galaxy groups using this study, in section 5.

An earlier volume limited sample, compiled during the WARPS project (Scharf et al. 1997) was deeper and resulted in 5 fossils in a redshift range of $z < 0.24$ with a space number density of $4 \times 10^{-6} h_{50}^3 \text{ Mpc}^{-3}$ (8-20% of all the systems with the same L_X). The 2dF fields (north and south) cover a total area of $\sim 1000 \text{ deg}^2$ which is about 14 times larger than the area covered in the WARPS X-ray survey, e.g. 73 deg^2 . Hence we probe a significantly larger volume in the present study than the X-ray selected WARPS sample. However, the $N_{gal} \geq 5$ selection criterion restricts us to richer galaxy systems, and results in a statistically well-controlled sample of 6 groups dominated by a luminous

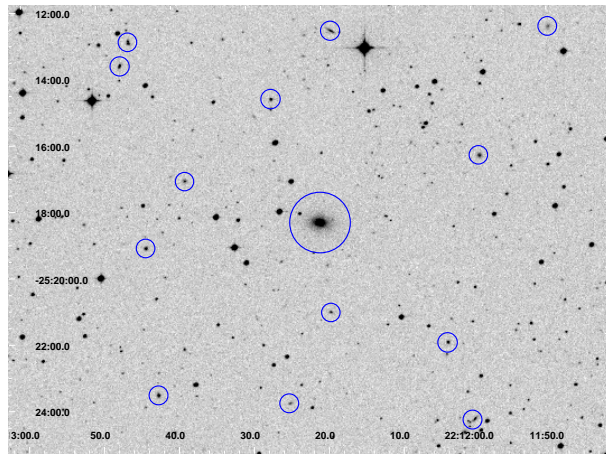


Figure 1. UKSTU Schmidt R-band image of the field of fossil candidate (2PIGG 2515) at $z \approx 0.062$ in 2dF south field. The circles show the group members with the dominant elliptical marked with larger circle at the centre of the field. The image is 12×12 arcmin².

elliptical galaxy, judged based on the optical data available at the time. Four of these systems have been observed by *Chandra*, within the area covered by 2PIGG catalog and up to $z=0.067$.

As mentioned briefly in the introduction, the major distinction between this sample and that of Rasmussen et al (2006) are the two additional constraints, e.g. the brightest galaxy in the group is as luminous as a giant elliptical galaxy and the presence of a large magnitude gap such that the giant elliptical galaxy appears relatively isolated. We note that the photometric data based on which we selected our sample was shallow and thus the morphological information may not have been accurate. In light of the new and deeper photometric observations, as part of this study, some galaxy properties appear to be different. We will return to this point later in sections 3 and 5.

2.1 X-ray observations

The main aim of the *Chandra* observations was to test for the presence of extended thermal X-ray emission associated with a hot intragroup medium, and to measure a mean gas temperature for all targets. The four targets were centred with the brightest group galaxy at the ACIS-S3 CCD aim-point and observed in VFAINT mode for nominal exposure times of 10–20 ks. These times were motivated by a desire to accurately constrain the mean hot gas temperatures within 5–10 per cent, based on the observed $L_X - L_B$ relation for X-ray selected fossils (Khosroshahi, Ponman & Jones 2007).

2.2 Optical observations

Optical observations of groups in this study were performed during two observing runs in December 2007, May 2008 using the 2.5 meter (100-inch) *Irénée du Pont* telescope, operating at Las Campanas Observatory. The telescope was calibrated with the wide field imager CCD (WFCCD) camera which covers a 25 arc-minute diameter field with a scale of 0.77 arcsec/pixel. The characteristic mean redshift of groups is $z \sim 0.06$ which corresponds to a luminosity distance

$D \sim 260$ Mpc and a scale of 1.13 kpc/arcsec, based on our cosmological assumptions.

For each galaxy group a total exposure time of 3600s and 1440s were applied in B-band and R-band respectively. Since each group image is a mosaic frame consisting of four individual pointing, the actual exposure time used for each group is one fourth of those values, i.e. 900s in B-band and 360s in R-band. To avoid pixel saturation due to bright sources and be able to remove cosmic rays as well as increasing the signal to noise, exposures were split into 300s and 120s in B-band and R-band, respectively. The photometric standards observations were also carried out at the time of the run with exposure times of 10 to 16 seconds in B-band and 4 to 8 seconds in R-band.

3 X-RAY ANALYSIS

The *Chandra* data were re-calibrated and analysed using CIAO v4.5 with CALDB v4.5.7. Bad pixels were screened out using the bad pixel map provided by the pipeline. Standard cleaning of background flares revealed no periods of significantly enhanced background in any of the data sets. Point sources were identified with the CIAO task 'wavdetect' and masked out in all subsequent analysis.

To search for the presence of extended X-ray emission, exposure-corrected surface brightness profiles were extracted from the BGG optical centre for each group. Due to the anticipated limited spatial extent and soft spectral nature of the sources, the background level was evaluated using a surrounding on-chip annulus. This ensures a reliable estimate of the local soft X-ray background. The resulting profiles are shown in Fig. 2. Despite displaying $\lesssim 200$ net counts each, three of the groups (2PIGG 1635, 2515 and 2868) show clear evidence ($> 3\sigma$ significance) for extended emission, with only 2PIGG 1404 remaining X-ray undetected. The detected emission extends to projected radii of $\gtrsim 50$ –100 kpc ($\gtrsim 0.8' - 1.5'$) in all three cases. This is well beyond the width of the *Chandra* point spread function as well as the BGG optical extent, strongly suggesting the presence of intragroup emission. In Fig. 2 we show the optical extend of the

2PIGG ID	RA (J2000)	Dec (J2000)	z	M_B	σ_v km/s	R_{vir} kpc	$M_{halo,dyn}$ $10^{12} h^{-1} M_\odot$	t_{obs} ks
1404	13 45 39.8	-05 30 33	0.052	-21.9	218	532	22.5	10
1635	00 16 25.8	-27 07 05	0.056	-21.8	189	461	11.6	20
2515	22 12 20.7	-25 18 29	0.062	-21.6	268	653	37.4	20
2868	03 14 33.1	-34 07 42	0.067	-22.2	213	520	25.2	10

Table 1. Properties of the 4 galaxy groups observed by *Chandra*. The coordinates refer to the position of the brightest galaxy in the group. The proposed exposure time is based on the expected fluxes to accumulate at least 1000 count per target using the $L_X - L_{opt}$ relation in Khosroshahi, Ponman & Jones (2007) for fossil groups. Column (9) gives a dynamical estimate for the halo mass from the group velocity dispersion given in column (6). The sample is complete out to $z = 0.07$ noting that only groups with at least 5 spectroscopically identified members are included.

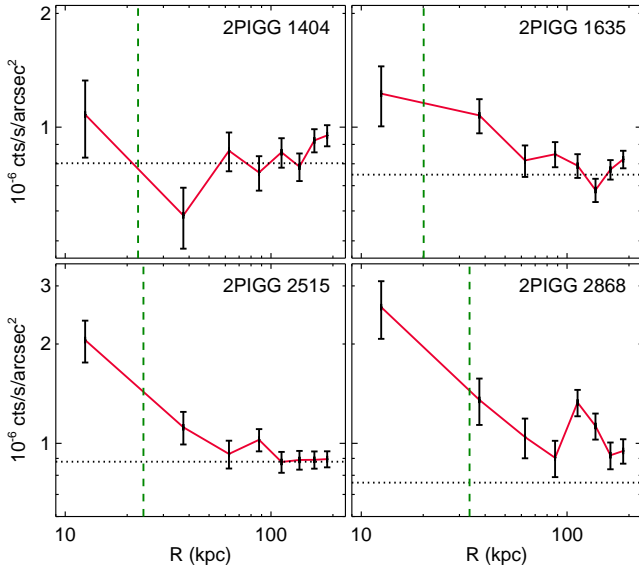


Figure 2. *Chandra* 0.3–2 keV X-ray surface brightness profiles of the groups. The horizontal dotted lines show the background level evaluated from a surrounding annulus in the source data. The vertical dashed lines mark the isophotal radius reaching 25 mag arcsec $^{-2}$ in B-band, e.g. $0.5 D_{25}$, for the brightest group galaxy. The X-ray surface brightness extends well beyond the optical size (D_{25}) of the most luminous galaxy in the group with the exception of 2PIGG 1404.

BGGs quantified using D_{25} , e.g. the isophotal diameter at the surface brightness of 25 mag arcsec $^{-2}$ in B-band, with values given in Table 3. Except for the 2PIGG 1404, the X-ray surface brightness extends beyond the corresponding isophotal radius. Fig. 3, which shows R-band optical images of our four groups (cf. Section 2.2) with smoothed X-ray contours overlaid.

Although all three X-ray detected groups are rather X-ray faint, useful constraints on the spectral nature of their X-ray emission could still be obtained. The spectral analysis assumed an APEC hot plasma emission model at the source redshift, absorbed by the Galactic H I column density at the relevant sky position (Kalberla et al. 2005). Given the limited photon statistics, the plasma abundance was fixed at an assumed value of $0.4 Z_\odot$ in all cases. Spectra were extracted within $R = 100$ kpc apertures ($R = 200$ kpc for 2PIGG 2868, cf. Fig. 2), accumulated in bins of ≥ 20 counts, and fitted

in XSPEC v12.8 assuming χ^2 statistics. Again, surrounding on-chip annuli were used for background estimation. In all cases, an APEC model was found to provide a better fit than a power-law, thus testifying to the thermal nature of the emission. To test the robustness of the spectral fitting for these low-surface brightness systems, we also obtained spectra in bins of just ≥ 5 net counts and fitted them assuming Cash statistics. In addition, we assumed an APEC spectrum and inferred X-ray temperatures from imaging data alone, using exposure-corrected (0.5–1)/(1–2) keV hardness ratios. Encouragingly, all three methods produced consistent temperature estimates for each of the three groups, lending credibility to the results.

Table 2 summarises the observational characteristics and derived X-ray properties for all four targets, including 1σ uncertainties on spectral parameters. For the X-ray undetected 2PIGG 1404, a 3σ upper limit on L_X is quoted, obtained from its count rate Poisson error and assuming $T = 1.0$ keV. In summary, the imaging and spectral analyses present a coherent picture in which three of the four target groups display extended, $T \approx 1$ –2 keV thermal emission with bolometric $L_{X,bol}$ in the range $(0.3$ – $2) \times 10^{42}$ erg s $^{-1}$. To allow straightforward comparison to the Jones et al. (2003) X-ray criterion for fossils, we also extrapolated the inferred luminosities out to $0.5 R_{vir}$, taking R_{vir} from Table 1. For a standard β -model for the surface brightness with $\beta = 0.5$ and $r_c = 20$ kpc, this would increase the luminosities quoted in Table 2 by a modest 10–70 per cent.

4 OPTICAL PROPERTIES

While the primary aim of the deep optical observations was to obtain a more accurate view of the groups and the brightest group galaxy, we also needed to obtain total optical luminosity of the galaxies in groups through photometric means. As a byproduct of this analysis we also obtain the galaxy luminosity function for future studies.

4.1 Star-galaxy separation

The imaging data for all 4 groups were reduced using IRAF Packages. Objects in all images were detected by SExtractor (Bertin & Arnouts 1996). Each detected object in the image catalogs is associated with a FLAG value which shows the degree of reliability of the measurements. After some iteration, we included all catalog entries with $FLAG \leq 3$, given

2PIGG ID	t_{exp} (ks)	R (kpc)	counts	S/N	N_{H} (10^{20} cm^{-2})	T (keV)	Z (Z_{\odot})	$L_{\text{X},0.3-2 \text{ keV}}$ ($10^{41} \text{ erg s}^{-1}$)	$L_{\text{X,bol}}$ ($10^{41} \text{ erg s}^{-1}$)	$L_{\text{X,bol}}(\leq r_{500})$ ($10^{41} \text{ erg s}^{-1}$)
1404	10.7	100	−6	0.0	1.84	1.0*	0.4*	< 1.3	< 2.1	< 2.1
1635	19.4	100	69	3.5	3.04	$1.6^{+1.7}_{-0.6}$	0.4*	1.4 ± 0.2	2.5 ± 0.3	4.7 ± 0.6
2515	19.9	100	73	3.7	1.99	$1.1^{+0.3}_{-0.2}$	0.4*	1.7 ± 0.2	2.7 ± 0.3	4.7 ± 0.5
2868	9.9	200	197	7.6	1.95	$2.2^{+1.1}_{-0.4}$	0.4*	10.1 ± 1.5	19.1 ± 2.9	26.9 ± 4.1

Table 2. Derived X-ray properties of the target groups: Cleaned exposure times t_{exp} , radius R of the circular aperture used for extraction of X-ray properties, 0.3–2 keV net counts and signal-to-noise (S/N) ratios, Galactic absorbing column N_{H} , and spectral parameters including pseudo-bolometric (0.05–10 keV) luminosities. Asterisk indicates an assumed value.

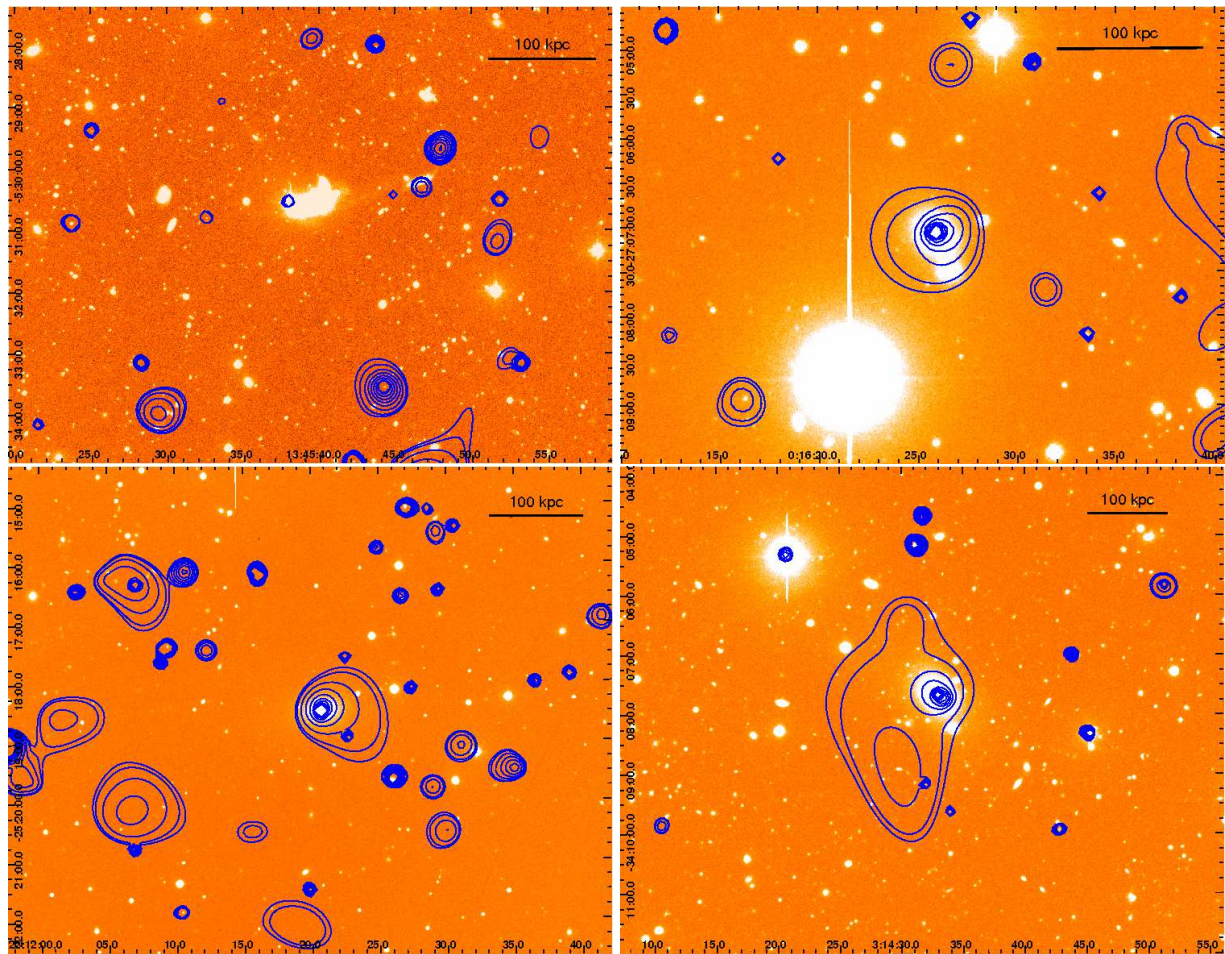


Figure 3. The smoothed X-ray contours over optical R-band images of the central regions. The images are 2PIGG 1404, 1635, 2515 and 2868 from left to right and top to bottom, respectively. Three out of the four groups show signatures of extended X-ray emission. See Fig. 7 for the zoomed in optical image of the core of 2PIGG 1404 for which we find no extended X-ray emission.

the quality of the photometric data and our desire to not exclude genuine galaxies. Catalogue entries with $\text{FLAG} > 3$ constitute to only ~ 2 per cent of the total number of entries.

Each entry in the catalogue also includes a stellarity class parameter, STAR , with values from 0 to 1. Lower the value, the more likely the detected object is an extended source, e.g. galaxy. The images and the radial profile of a number of objects with different values of STAR parameter were examined in IRAF before deciding the borderline.

Typically, objects with $\text{STAR} > 0.83$ were found to be stars, whilst those with ≤ 0.83 were galaxies.

4.2 Photometric completeness

As an example, the completeness level of the B- and R-band photometric data for 2PIGG 2868 is shown in Fig. 4. The solid and the dashed histograms show the magnitude distribution of the galaxies in the field in R- and B-band, respectively. The adopted magnitude limit in the R-band is shown

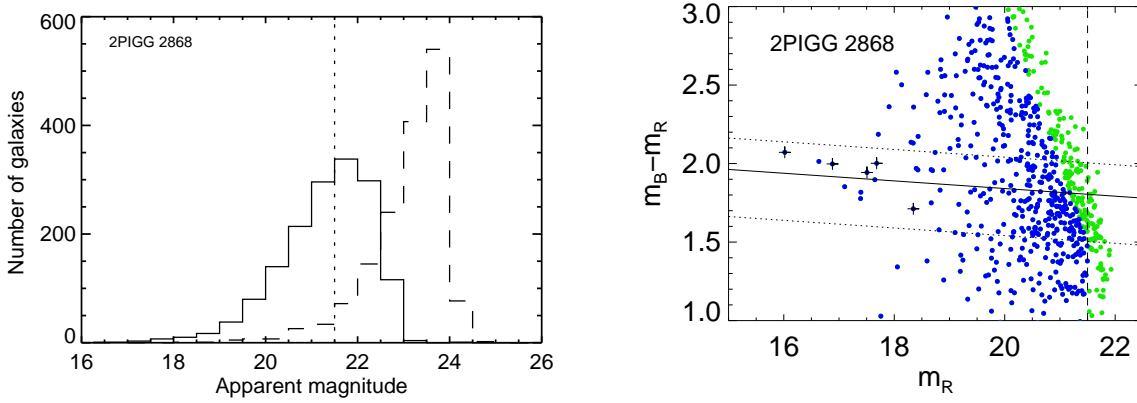


Figure 4. Left: An example magnitude histogram of galaxies for 2PIGG 2868 in the R-band (solid) and the B-band (dashed). Right: Colour magnitude diagram of galaxies in the observed fields of view of 2PIGG 2868. The crosses mark the spectroscopically confirmed group members. The dark/blue filled circles show galaxies within the field of view within the applied R- band and B- band magnitude completeness limit. The gray/green filled data points mark galaxies in the observed field of view but outside the magnitude completeness limit. The solid black line is a linear fit to all spectroscopically confirmed group members while the upper and lower lines are the 2σ confidence levels (dotted lines), within which the galaxies are assumed to be the group members.

by a vertical dashed line. This limit was determined considering the position of the peak in the apparent magnitude histogram for each group.

4.3 Colour-magnitude diagram and group membership

In the absence of spectroscopic redshift measurements, the colour magnitude diagram (CMD) is often used to assign galaxies to groups, in particular since early-type galaxies form a red sequence which is a characteristic of their evolution (e.g. Kodama & Arimoto 1997).

The total apparent magnitude and magnitude within an aperture of 5 arcsec were obtained in both R- and B-band filters. The $m_B - m_R$ colour for all objects identified as galaxies within a virial radius is presented against the total apparent magnitude in Fig. 4. The spectroscopic members based on the redshift of galaxies around the BGG within the virial radius of groups were also found using the NED data base and the 2dF galaxy redshift survey. Galaxies were assigned as spectroscopic group members if they fall within a redshift range of $0.005 \times (1 + z_g)$ from BGG redshift (Finoguenov et al. 2010).

As an example, Fig. 4 shows the CMD of 2PIGG 2868, with crosses representing spectroscopic group members. The blue points are all galaxies within field of view after applying the R- and B-band magnitude completeness. The solid line is a linear fit to all spectroscopic early type galaxy members while the two lower and upper lines are $\pm 2\sigma$ confidence levels.

4.4 Galaxy luminosity function

The study of the luminosity function of galaxies in different environments provide important observational constraints for cosmology and galaxy formation and evolution models. Schechter (1976) and Turner & Gott (1976) determined

the galaxy luminosity functions of groups and rich clusters. Schechter (1976) also proposed the following form for the luminosity function according to the observed data of clusters and field galaxies

$$\Phi(M)dM = (0.4\ln 10)\Phi^* X^{(1+\alpha)} \times \exp^{-X} dM \quad (1)$$

where $X = 10^{0.4(M^* - M)}$ and the quantity $\Phi(M)$ is proportional to the number of galaxies that have absolute magnitudes in the range $(M, M+dM)$, Φ^* is the characteristic number density, M^* is the characteristic absolute magnitude.

At the bright end, the Schechter function drops sharply. It rises at the faint-end following a power law with a slope given by α . Thereby, the faint-end slope is decreasing, increasing, or flat for $\alpha > -1$, $\alpha < -1$, and $\alpha = -1$ respectively.

Galaxies were selected as group members on the basis of the estimated upper and lower confidence levels found in previous section from a linear fit to $m_B - m_R$ colour of groups members. Therefore, a $m_B - m_R$ colour cut-off was applied at $m_B - m_R = (-0.023 \pm 0.002) \times m_R + (2.327 \pm 0.034)$ where m_R is the apparent R-band magnitude of any object in the fields.

In addition, a statistical method of background subtraction was employed to remove the contamination from foreground-background objects. To obtain a background galaxy sample, regions beyond r_{200} radius in each group mosaic image were selected as a background field, roughly corresponding to an area of 1 deg^2 . For each group, the net galaxy luminosity function was determined by subtracting the normalised background luminosity function, from the luminosity function for the same group in the R-band.

The group R-band luminosity functions are shown in Fig. 5 for individual groups. The curve shows the single Schechter function fit on the luminosity function of group members. We excluded the BGG in the LF fitting, because the large luminosity gap results in a poor fit and poor constraint for M^* values. A single Schechter function of the

form of Eq. 1. yielding the best fitting values in R-band are given in Table 3.

We calculate the dwarf to giant ratio of our sample groups using their luminosity functions. We assume galaxies brighter than -19.0 mag as giants and dwarf galaxies, with absolute magnitude between -19.0 and -17.0 (or -16.0). Results for dwarf to giant ratio are presented in Table 3.

Two of the sample groups, 2PIGG 2515 and 2868, show a large magnitude gap (≥ 2 mag) between the second brightest galaxy within the half of the Virial radius and the BGG, in R-band. Although 2PIGG 1404 shows a magnitude gap of 1.6 mag, the BGG shows a disturbed morphology indicating that is in the process of merging with the second brightest galaxy and futures associated with on going merger are present. **The BGG in this case is not a giant elliptical galaxy.**

At the core of the group 2PIGG 1635 there is a bright galaxy close to the BGG with about 1 magnitude gap. In the absence of sufficient information to rule out projection effect, we assume that these two galaxies are in the pre-merger state. The reason this group was included in the candidate sample, in the first place, was poor photometric measurement based on which the 2dF galaxy redshift survey was built, at the distance of this group.

We also derived the composite luminosity function of the four galaxy group in R-band within Virial radius and half the Virial radius. The composite luminosity function has been constructed by combining the individual luminosity functions of four galaxy groups. Number of galaxies in each magnitude bin have been normalised to the total area of groups contributing in corresponded bin. Fig. 6 shows the composite luminosity function within r_{200} (left panel) and $0.5r_{200}$ (right panel). The dotted and dashed curves (left panel in Fig. 5) indicate the commonly-used Schechter function fits on the observed composite luminosity function including and excluding the BGGs, respectively. The best values of Schechter parameters in each fit have been computed as $M^* = 21.10 \pm 0.18$ (without BGGs), $M^* = 22.86 \pm 0.24$ (with BGGs), $\alpha = 1.32 \pm 0.02$ (without BGGs) and $\alpha = 1.48 \pm 0.03$ (with BGGs). The best Schechter function fit to the observed composite luminosity function of groups within half of the Virial radius (right panel in Fig. 5) with excluding the BGGs gives Schechter parameters as $M^* = 19.27 \pm 0.14$ and $\alpha = 0.72 \pm 0.07$.

4.5 A brief note on 2PIGG 1404

The brightest galaxies in all of the groups are giant elliptical galaxies except for the brightest galaxy in 2PIGG1404, which appears to exhibit disk like structure. This galaxy is slightly bluer (~ 0.2 mag) than the other brightest galaxies in the groups in our sample. A closer look at the surrounding of the BGG reveals a tidal interaction between this galaxy and its companion galaxy (Fig. 7). There is also a foreground stellar source which matches the location of the detected X-ray point source (Fig. 3, top-left). **Given the nature of this group in the optical, we argue that this galaxy group should not have been in our sample in the first place as the BGG morphology does not satisfy the initial selection criteria (condition II and III, section 2). As a result the major contrast between this**

galaxy group and the other groups in our sample is the BGG morphology.

5 DISCUSSION AND CONCLUSIONS

We carried out *Chandra* X-ray observations of a sample of 4 galaxy groups, each *appeared* to be dominated by a giant elliptical galaxy in b_J -band images, to explore whether they are also associated with a group scale X-ray emissions. If detected, one could provide a direct evidence that luminous elliptical galaxies form within the collapsed core of galaxy groups where the ionised gas reaches a ~ 1 keV temperature. The X-ray emission itself can be used to probe the gravitational potential of the group which is complementary to the dynamical mass estimation, often used for galaxy groups.

The X-ray analysis shows that, although the detected X-ray emission is primarily associated with the brightest group galaxies, there are clear evidences for the extended X-ray emission when the BGG is *genuinely* a giant elliptical galaxy. Our deep optical observations, following the X-ray observations, show that one of the BGGs is not a giant elliptical galaxy, despite what we had planned based on the optical observations available at the time and prior to the X-ray observations. We found 3 galaxy groups with giant elliptical BGGs to be associated with X-ray emission extending beyond the optical size of the BGG. One of these 3 galaxy groups (2PIGG 2868) meets the requirements for fossil groups, satisfying both the X-ray luminosity and the optical luminosity gap criteria, while two remaining galaxy groups marginally satisfy the X-ray luminosity within the measurement uncertainty, of which only one meets the optical criterion on the luminosity gap, noting that for the cosmology adapted in this study the conventional threshold for the X-ray luminosity is $0.5 \times 10^{42} h_{70}^{-2} \text{ erg s}^{-1}$.

In Fig. 8 we present $L_X : L_{opt}$ scaling relations for groups and galaxy sample in order to compare with our observations. The $L_{B,tot}$ and $L_{R,tot}$ refer to the group B- and R-band luminosity in solar luminosity units. As seen in this figure, the groups studied here follow the general trend of X-ray bright groups in Helsdon & Ponman (2003) but are dimmer in X-ray compared to the X-ray selected fossil groups in Khosroshahi, Ponman & Jones (2007). Fig. 9 compares the X-ray luminosity associated with early type galaxies as a function of their B-band optical luminosity, L_B , between Ellis & O'Sullivan (2006) sample and this study. Our sample galaxies are generally as X-ray luminous as the BGGs in other groups, for their optical luminosity.

The X-ray luminosity of the 2PIGG 2868 is $L_X = 1.9 \times 10^{42} \text{ erg s}^{-1}$ which clearly satisfies the X-ray criterion for fossils. Assuming a beta model for the X-ray surface brightness distribution with $\beta = 0.5$ and core radius, $r_c = 20$ kpc, the extrapolated X-ray luminosity will be $L_X(500) = 2.7 \times 10^{42} \text{ erg s}^{-1}$, within $r_{500} = 0.51$ Mpc, an increase by a factor of 1.41. For the estimation of r_{500} we use the observed X-ray temperature and scaling relation given by Sun et al. (2004). Despite this, as seen in Fig. 8, the group is dimmer in X-ray than what is expected from the scaling relations known for the X-ray selected fossils (Khosroshahi, Ponman & Jones 2007).

Another group, 2PIGG 2515, has an X-ray luminosity of $L_X = 2.7 \times 10^{41} \text{ erg s}^{-1}$. With the above assumptions on

2PIGG ID	M_B^{BGG}	M_R^{BGG}	$B-R^{BGG}$	$\Delta m_{12}^{0.5vir}$	D_{25}^{BGG} (kpc)	M_R^*	α	$\frac{N_{Dwarf}^I}{N_{Giant}^I}$	$\frac{N_{Dwarf}^{II}}{N_{Giant}^{II}}$
1404	-21.0	-22.6	1.8 ± 0.1	1.6	45.2	-21.73 ± 0.46	-1.57 ± 0.06	2.2	5.3
1635	-20.8	-22.7	2.0 ± 0.1	1.1	40.2	-19.42 ± 0.36	-1.12 ± 0.10	2.2	4.1
2515	-21.3	-23.4	2.1 ± 0.1	3.4	47.9	-22.10 ± 0.52	-1.28 ± 0.06	1.5	—
2868	-21.2	-23.1	2.0 ± 0.1	2.5	67.3	-22.15 ± 0.48	-1.59 ± 0.06	2.1	5.0

Table 3. Optical properties of the sample groups. Column (2) to (4) are our measured BGG magnitudes in B- and R-bands and B-R colour, respectively. **Column (5) gives the diameter, D_{25} , of the BGG in kpc reaching the surface brightness of 25 mag/arcsec² in B-band.** Column (6) and (7) are the R-band galaxy luminosity function parameters from a single Schechter fit. Dwarf to giant ratios are also given in the last two columns, (I) Giants: $M_R \leq -19$ and Dwarfs: $-19 \leq M_R \leq -17$), (II) Giants: $M_R \leq -19$ and Dwarfs: $-19 \leq M_R \leq -16$).

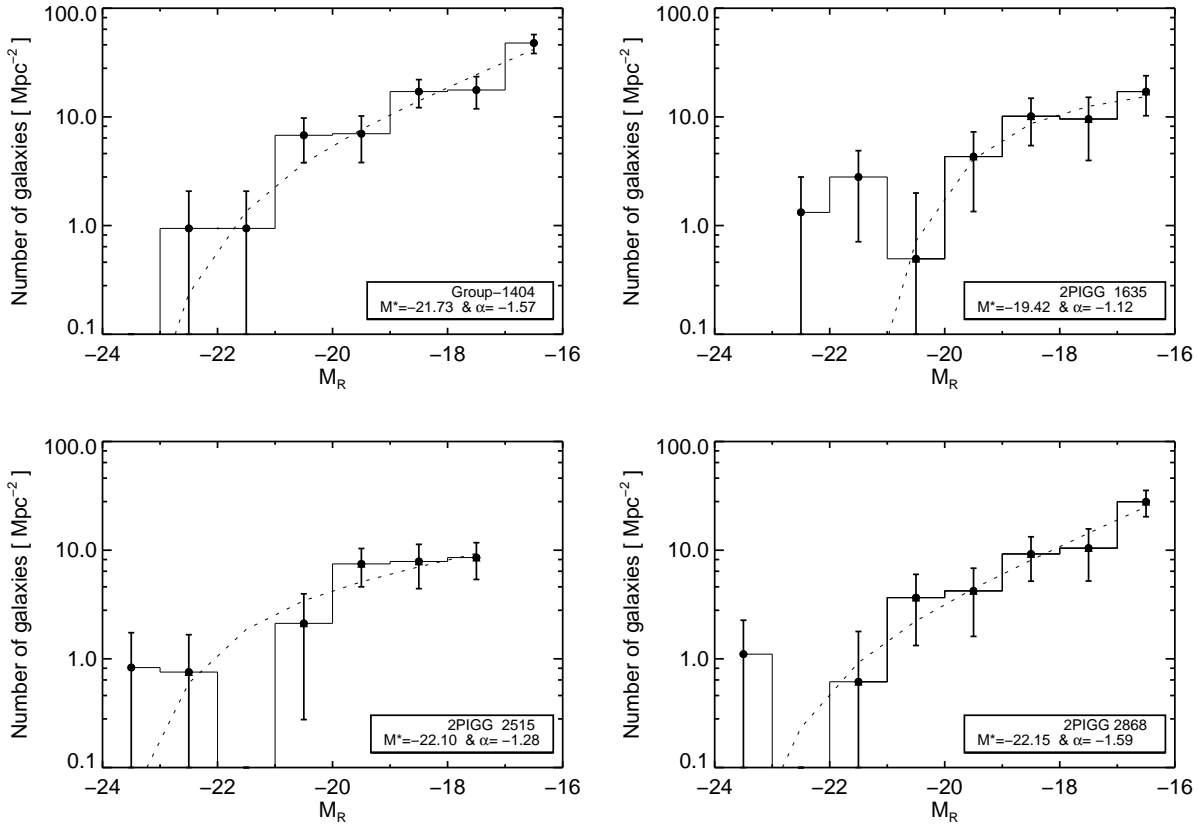


Figure 5. The galaxy luminosity function for the sample groups, 2PIGG 1404, 1635, 2515 and 2868 from left to right and top to bottom. The fitted Schechter parameters are also given for each luminosity function.

the X-ray surface brightness profile, we obtain an extrapolated bolometric luminosity of $L_X(500) = 4.7 \times 10^{41} \text{ erg s}^{-1}$, within $r_{500} = 0.34$ Mpc, a factor of 1.75 increase compared to the measured X-ray luminosity. Within the measurement uncertainty, this group satisfies the fossil X-ray luminosity limit. The same applies to 2PIGG 1635 for which we find an extrapolated X-ray luminosity of $L_X = 4.7 \times 10^{41} \text{ erg s}^{-1}$. However, based on higher quality imaging obtained in this study, this system does not meet the requirement for large luminosity gap and thus can not be classified as a fossil group.

As outlined in the introduction, the main aim of this study was to test the hypothesis that the collapsed core of

the galaxy groups is a suitable environment for the build up of giant elliptical galaxies. Admitting the statistical limitation of the sample, this study supports the hypothesis by demonstrating that groups possessing a giant elliptical BGG, are associated with an extended X-ray emission. A more rigours test requires a statistically larger sample. In this study we demonstrate that the diffuse X-ray emission is detected in 3 out of the 4 targeted groups. For these 3 groups, the observed X-ray luminosity is 2 to 4 times the expected X-ray luminosity from typical galaxy groups. Thus, within the statistical uncertainty, it appears that giant elliptical galaxies form within the collapsed core of galaxy groups.

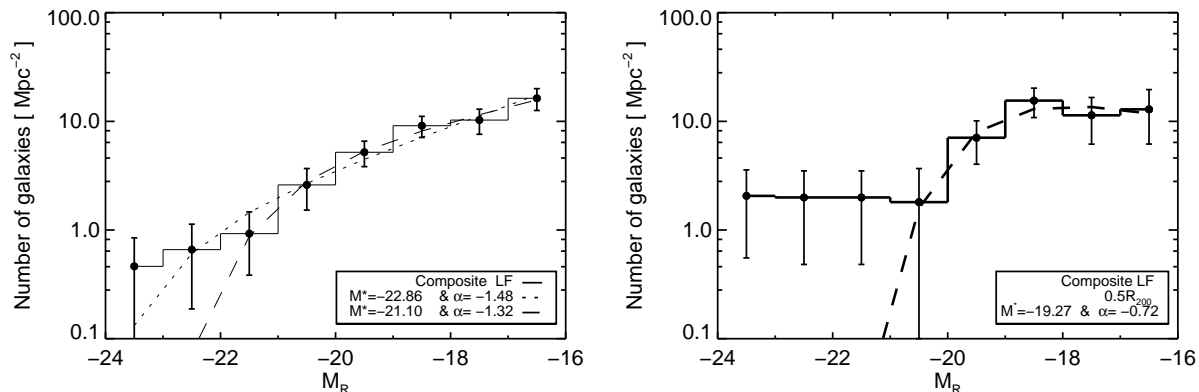


Figure 6. The composite luminosity function of four groups in our sample, within the r_{200} radius (left) and $0.5 r_{200}$ (right). The dotted and dashed curves indicate the Schechter function fits to the observed composite luminosity function including and excluding the BGGs, respectively.

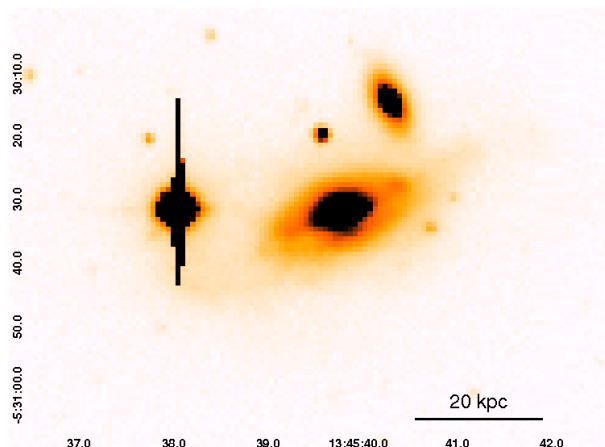


Figure 7. A zoomed in R-band image of the 2PIGG 1404 showing a disturbed morphology of the brightest group galaxy indicating an ongoing tidal interaction with its nearest galaxy.

With these findings and with the caveat that we have only selected galaxy groups with at least 5 spectroscopically confirmed members, we can obtain a rough estimation for the number density of optically identified fossil groups. As described in (Jones et al. 2003) the number density of X-ray selected fossil groups with $L_X \geq 0.5 \times 10^{41} h_{70}^{-2} \text{ erg s}^{-1}$ is found to be $\approx 11^{+7.4}_{-4.9} \times 10^{-6} h_{70}^3 \text{ Mpc}^{-3}$, adapted to the cosmology assumed here. This is 10 times the number density of rich galaxy clusters (Jones et al. 2003).

The 2PIGG galaxy groups catalog covers a total area of $\approx 1400 \text{ deg}^2$ in north and south stripes of the 2dFGRS and the observed sample of groups in this study is complete out to $z = 0.067$ (Table 1). The total comoving volume of the survey corresponds to $3 \times 10^6 \text{ Mpc}^3$, at this redshift. Thus the number density of fossil groups is calculated to be $\approx 3 - 7 \times 10^{-7} h_{70}^3 \text{ Mpc}^{-3}$, assuming that only 1 (or at most 2) of the observed groups meet the fossil X-ray criteria. This is 20 to 40 times less than the fossil number density found in the WARPS project, which was built on serendipitous X-ray sources from ROSAT Pointed observations (Jones et al. 2003) and 5 to 10 times less than the

number density estimate based on the Millennium cosmological simulations Dariush et al. (2007), which is reported to be $\approx 35 \pm 1 \times 10^{-7} h_{70}^3 \text{ Mpc}^{-3}$. However, we note that, as referred to in section 2, the $N_{gal} \geq 5$ criterion only allows a small fraction of galaxy groups with a large luminosity gap to be selected for X-ray follow-up. Relaxing the restriction on N_{gal} , but retaining our other selection criteria described in section 2 (the luminosity gap and the BGG luminosity), we find a total of 48 groups within $z=0.067$, as compared to 4 groups selected for the X-ray follow-up. Assuming only 25 to 50 percent of the groups meet fossil groups criteria, the number density of fossil groups is estimated to be 4 to $8 \times 10^{-6} h_{70}^3 \text{ Mpc}^{-3}$, nearly equal to the Millennium simulations estimate and only half the space density obtained from the X-ray selected sample (Jones et al. 2003). We note the statistical limitation of the sample and thus the values should be taken as a rough estimation.

Finally, to highlight an interesting feature of fossil groups, Fig. 10 shows a comparison between a sample of galaxy groups (Osmond & Ponman 2004), X-ray selected fossils (Khosroshahi, Ponman & Jones 2007) and the ob-

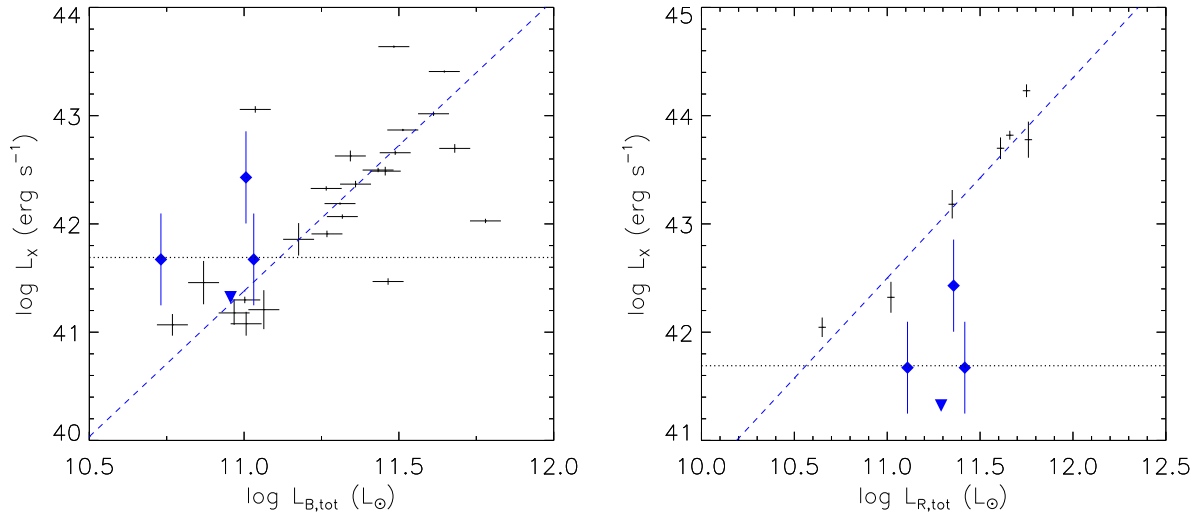


Figure 8. The $L_{opt} : L_X$ relation for the optically selected groups in this study (dark/blue symbols) and the X-ray bright groups (Helsdon & Ponman 2003) (left) and the X-ray selected fossil groups (Khosroshahi, Ponman & Jones 2007) (right). The $L_{B,tot}$ and $L_{R,tot}$ refer to the total B- and R-band luminosity of the group. The fitted dashed line is the best fit to the presented comparison data. The dark/blue triangle represents 2PIGG 1404 for which only an upper limit X-ray flux is available.

served sample of optically selected groups in the plane of $T_X : \sigma$ relation. As seen, some of our sample groups, the fossils in particular, have a hotter IGM for the group velocity dispersion. This relatively higher IGM temperature observed in optically selected groups could also support the argument that the core of these groups are collapsed. Deeper X-ray observations and complementary spectroscopic membership identification can reveal the true nature of the optically selected groups with a dominant giant elliptical galaxy.

Acknowledgement: We wish to thank Alexis Finoguenov for his useful comments and the anonymous referee for comments and suggestions that helped us improve the presentation and the discussion of this manuscript.

REFERENCES

- Adami, C., Russeil, D., Durret, F., 2007b, *A&A*, 467, 459
 Alshino, A., Khosroshahi, H., Ponman, T., et al. 2010, *MNRAS*, 410, 941
 Bertin E., Arnouts S. 1996, *A&AS*, 117, 393
 Colless, M. 1989, *MNRAS*, 237, 799
 Dariush A. A., Khosroshahi H. G., Ponman T. J., Pearce F., Raychaudhury S., Hartly W., 2007, *MNRAS*, 382, 433
 Dariush A. A., Raychaudhury S., Ponman T. J., Khosroshahi H. G., Benson A. J., Bower R. G., Pearce F., 2010, *MNRAS*, 405, 1873
 Dunkley J., Komatsu, E., Nolte, M. R., et al. 2009, *ApJS*, 180, 306
 Eke, V.R.; Baugh C.M.; Cole S., et al. 2004, *MNRAS*, 348, 866
 Ellis, S. C.; O’Sullivan, Ewan, et al. 2006, *MNRAS*, 367, 627
 Finoguenov, A., Watson, M., G., Tanaka, M., et al. 2010, *MNRAS*, 403, 2063
 Girardi M., Giuricin G., Mardirossian F., Mezzetti M., Boschin, W. 1998, *ApJ*, 505, 74
 Gozaliasl, G., Finoguenov A., Khosroshahi H. G., et al, 2013, submitted to *A&A*
 Helsdon, S. F., Ponman, T. J., 2003, *MNRAS*, 340, 485
 Kalberla P. M. W., Burton W. B., Hartmann D., Arnal E. M., Bajaja E., Morras R., Pöppel W. G. L., 2005, *A&A*, 440, 775
 Khosroshahi H.G., Jones L.R., Ponman T.J. 2004, *MNRAS*, 349, 1240
 Khosroshahi H.G., Maughan B.J., Ponman T.J., Jones L.R. 2006, *MNRAS*, 369, 1211
 Khosroshahi H. G., Ponman T. J., and Jones L. R., 2006, *MNRAS Letters*, 372, 68
 Khosroshahi H.G., Ponman T.J., Jones L.R. 2007, *MNRAS*, 377, 595
 Khochfar S., Burkert A., 2005, *MNRAS*, 359, 1379
 Kodama, T., Arimoto, N. 1997, *A&A*, 320, 41
 Jones, L. R., Ponman, T. J., Horton, A., et al. 2003, *MNRAS*, 343, 627
 Lin, Y. T., Mohr, J. J., Stanford, S. A. 2004, *ApJ*, 610, 745
 Miller, C. J., et al 2005, *AJ*, 130, 968
 Milosavljevic, M., Miller C. J., Furlanetto R., Cooray A. 2006, *ApJ*, 637, 9
 Miraghaee H., Khosroshahi, H.G., Klockner, H.R., Jetha, N. N., Raychaudhury, S., Ponman, T.J., 2013, *MNRAS*, submitted
 Osmond J.P. F. and Ponman T. J., 2004, *MNRAS*, 350, 1511
 O’Sullivan E., Forbes D. A., Ponman T. J., 2001, *MNRAS*, 328, 461
 Ponman T. J., Allan D. J., Jones L. R., Merrifield M., MacHardy I. M., 1994, *Nature*, 369, 462
 Popesso, P., Biviano, A., Bhinger, H., Romaniello, M., Voges, W. 2005, *A&A*, 433, 431
 Rasmussen J., Ponman T.J., Mulchaey J. S., Miles T. and Raychaudhury S., 2006, *MNRAS*,
 Santos W. A., Mendes de Oliveira C., Sodre L. Jr., 2007,

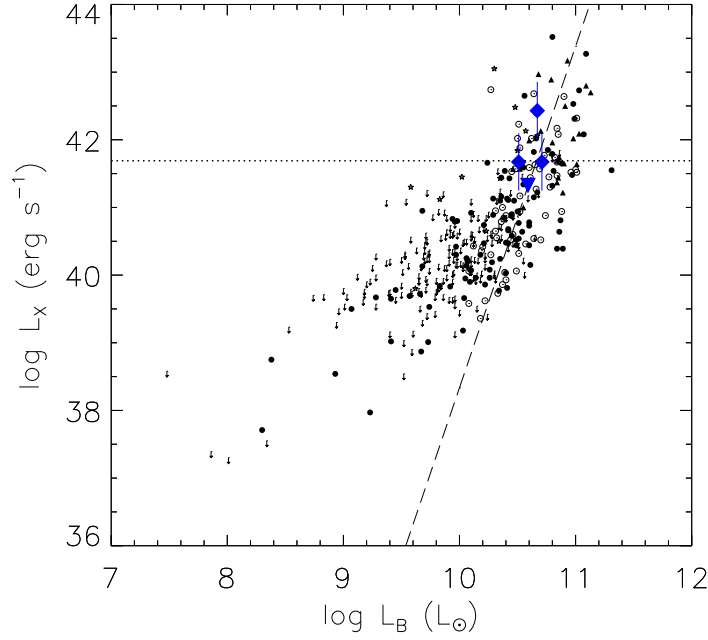


Figure 9. A comparison between brightest group galaxies in our sample and the various early type galaxies in Ellis & O’Sullivan (2006) in the plane of $L_X : L_B$. The L_B refers to the B-band luminosity of the galaxies. The symbols are the same as in their Fig. 2, triangles for BCGs, open circles for BGGs, stars for AGN, arrows indicating the upper limits for any type and filled circles are other types of galaxies. The dashed line is the best fit for the $L_X : L_B$ associated with the BGGs in their sample. The X-ray luminosity of the groups for which we detect extended X-ray emission, all except 2PIGG 1404, have been extrapolated to their r_{500} . The horizontal dotted line marks the fossil X-ray threshold as given by Jones et al. (2003). Three of the groups show L_X above or close to this threshold.

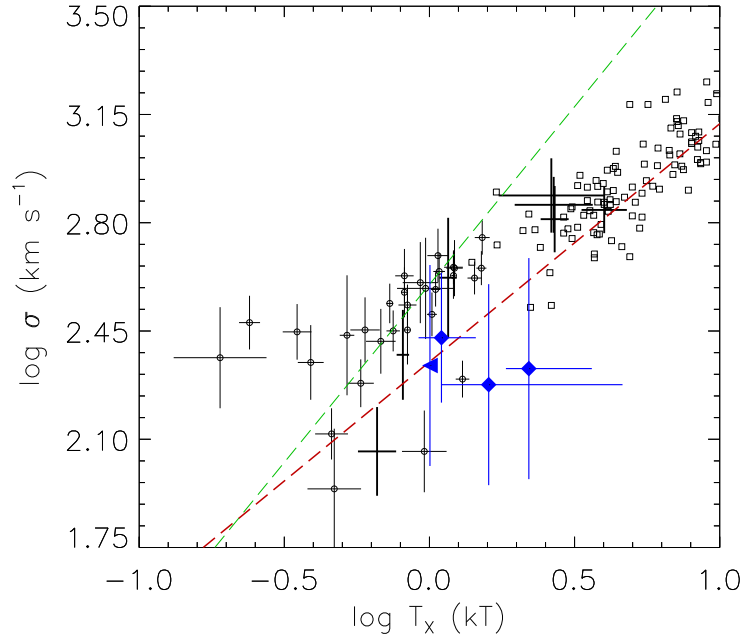


Figure 10. The $T_X : \sigma$ relation for the optically selected groups in this study (dark/blue symbols) and the X-ray selected fossil groups (Khosroshahi, Ponman & Jones 2007) (black bold), GEMS galaxy groups (Osmond & Ponman 2004) (open circles; best fit green dashed line) and galaxy clusters (Wu, Xue & Fang 1999) (open squares; best fit red dashed line). The dark/blue triangle represents 2PIGG 1404 for which we assume 1 keV temperature in spectral fitting.

- AJ, 134, 1551
 Schechter P. 1976, ApJ 203, 297
 Scharf C. A., Jones L. R., Ebeling H., Perlman E., Malkan M., Wegner G., 1997, ApJ, 477, 79
 Smith G.P., Khosroshahi H.G., Dariush A., Sanderson A. J. R., Ponman T. J. , Stott J. P. , Haines C. P. , Egami E. , Stark D. P. , 2010, MNRAS, 409, 169
 Springel et al., 2005, Nature, 435, 629
 Sun, M.; Forman, W.; Vikhlinin, A.; Hornstrup, A.; Jones, C.; Murray, S. S., 2004, ApJ 612 , 805
 Sun, M.; Voit, G. M., Donahue M, Jones C., Forman W., Vikhlinin A., 2008, ApJ 693 , 1142
 Tavasoli, Saeed; Khosroshahi, Habib G.; Koohpae, Ali; Rahmani, Hadi; Ghanbari, Jamshid, 2011,PASP,123,1
 Turner, E.L. & Gott, J.R., 1976, ApJ, 209, 6
 Ulmer, M. P.; Adami, C.; Covone, G.; Durret, F.; Lima Neto, G. B.; Sabirli, K.; Holden, B.; Kron, R. G.; Romer, A. K., 2005, ApJ 624 , 124
 Wechsler, Risa H.; Bullock, James S.; Primack, Joel R.; Kravtsov, Andrey V.; Dekel, Avishai
 Wu X.-P., Xue H., & Fang L.-Z. ,1999, ApJ, 524, 22